Research Square

Preprints are preliminary reports that have not undergone peer review.
They should not be considered conclusive, used to inform clinical practice,
or referenced by the media as validated information.

NE/β2-AR Promotes Directional Migration of Colorectal Cancer Cells to the Liver by Inducing M2 Polarization of Kupffer Cells and Upregulating CXCL12 Expression

Xiaoyan Li
the Third Department of Oncology of Hebei General Hospital
Na Yuan
the Third Department of Oncology of Hebei General Hospital
Ce Zhou
the Fourth Department of Cardiovascular of Hebei General Hospital
Jie Zhi
the Third Department of Oncology of Hebei General Hospital
Yang Li
the Third Department of Oncology of Hebei General Hospital
Bin Wang
the Third Department of Oncology of Hebei General Hospital
Wujie Zhao
the Third Department of Oncology of Hebei General Hospital
Yitao Jia (jiayitao99@163.com)
the Third Department of Oncology of Hebei General Hospital

Research Article

Keywords: Colorectal cancer, Liver metastasis, Kupffer cells, Norepinephrine, PI3K/Akt, CXCL12

Posted Date: December 20th, 2021

DOI: https://doi.org/10.21203/rs.3.rs-1111190/v1

License: This work is licensed under a Creative Commons Attribution 4.0 International License.
Read Full License

Abstract

Background and Aim The exact mechanism of colorectal cancer (CRC) liver metastasis remains unclear. This study aimed to explore the role and mechanism of the norepinephrine (NE) in the directional migration of CRC cells to the liver.

Methods In mouse models of CRC liver metastasis, the effects of NE on the number of liver metastases and the density of intrahepatic Kupffer cells (KCs) were observed. *In vitro* experiments were performed to detect KC polarization markers by flow cytometry, cytokines by enzyme-linked immunosorbent assay (ELISA), migration of colon cancer cells by Transwell migration assay, AR expression and PI3K/Akt signaling pathway-related protein expressions by Western blotting, and chemokine mRNA expressions by reverse transcription-polymerase chain reaction (RT-PCR).

Results Two weeks after intraperitoneal injection of different doses of NE in CRC liver metastasis mouse models, the number of liver metastases were (111.00±51.43) and (102.40±54.85) in the low-dose (0.28 nmol) NE group and high-dose groups (2.8 nmol), respectively, which were significantly higher than those in the control group (both P 0.05); in addition, the density of intrahepatic KCs in the NE group was significantly reduced compared with the control group (P<0.05). *In vitro* experiments showed that low-concentration NE induced M2 polarization of KCs; NE upregulated the expression level of NE receptor β_2-AR on KCs and activated the PI3K/Akt pathway, while blocking β_2-AR or using a PI3K inhibitor inhibited this process (P< 0.05). M2 KCs promoted the migration of colon cancer cell line CT26. Eight macrophage-associated chemokines were screened from the TISIDB website. CXCL12 expression in KCs was significantly higher in low-concentration (10^{-9} M) NE group than in controls, and a β2-AR blocker down-regulated CXCL12 expression in KCs (both P < 0.05).

Conclusions NE/β_2-AR may induce intrahepatic KC M2 polarization through the PI3K/Akt pathway and promote its secretion of CXCL12 to induce the directional migration of CRC to the liver. Our findings provide important evidence in the search for new strategies to prevent liver metastasis from CRC.

Introduction

Colorectal cancer (CRC) is the third most common cancer and the second most common cause of cancer-related death globally.[1] Due to a variety of reasons, most CRC patients are already in the advanced stages when they are diagnosed, and 15%-25% of them have liver metastases.[2] The rate of liver metastases can reach 50% throughout the course of CRC, and the median survival time for patients with untreated liver metastases is only 6.9 months.[3] The main treatment options for liver metastases from CRC currently include surgery, radiotherapy, chemotherapy, and molecularly targeted therapy; however, more than half of patients will experience recurrence of colorectal liver metastases within 2 years.[4] Therefore, compared with the treatment of liver metastases, preventing or reducing the occurrence of liver metastases will help improve the prognosis of CRC patients.

Clinically, it is common that the incidence of liver metastases found during the follow-up period varies considerably among CRC patients in the same stage and receiving the same treatment, which highlights the potential role of the microenvironment of the target organ in the body.[5] The liver is not only the largest digestive and metabolic organ but also a very important part of the immune system.[6] A variety of cells including liver sinusoidal endothelial cells, Kupffer cells (KCs), hepatocytes, myeloid-derived suppressor cells (MDSC), and tumor-associated neutrophils (TAN) interact to form a complex immune microenvironment and jointly participate in the immune regulation of the liver.[7] KCs were liver-resident macrophages located in hepatic sinusoids, accounting for 80-90% of the monocyte-macrophage cell system. The functions of KC can be influenced by a variety of factors including endotoxin, lipopolysaccharide, and stress.[8] When activated, KCs can produce a variety of cytokines such as vascular endothelial growth factor (VEGF), TGF-β, IL-6, and TNF-α, thus exerting biological effects (e.g. killing effect).[9] It has been found that NOTCH signaling promotes intrahepatic KC polarization towards M2 macrophages, which ultimately promotes CRC liver metastasis.[10]

The interaction between the liver and the intestine, known as the "liver-gut axis", are always present under both pathological and physiological states. For example, intestinal flora disorders can induce inflammatory responses and fibrosis in the liver, leading to cirrhosis and hepatic encephalopathy.[11] In addition, abnormal gut flora can affect the occurrence of liver metastases from CRC.[12] There is growing evidence that neurons and their neurotransmitters play an important role in CRC liver metastasis.[13] The levels of the stress-related hormone NE and its β-adrenergic receptor (β-AR) dramatically increase in CRC tissue and are strongly associated with poor prognosis in CRC patients.[14, 15] Further studies have revealed that β-AR is also widely expressed on immune cells and can influence the immune microenvironment of tumours by regulating the function of immune cells and thus affect tumor occurrence and progression .[16] Activation of β2-AR reduces the infiltration of CD8+ CTL cells in the tumor microenvironment and inhibits the activation of CD8+ T cells; NE also inhibits the cytotoxicity of NK cells and reduces the secretion of IFN-γ through the β2-AR/cAMP/PKA/p-CAEB pathway; activation of the β_2-AR pathway promotes STAT3 phosphorylation, which in turn significantly increases the survival of MDSCs in the tumor microenvironment and enhances their immunosuppressive function, ultimately promoting tumor progression.[17–19] To date, it is still unclear whether and how NE can affect the development of CRC liver metastases. This study aims to explore the potential role and mechanism of the enteroneurotransmitter NE during CRC liver metastasis, in order to provide evidence for establishing new prevention and treatment strategies of CRC liver metastasis.

Materials And Methods

Animal experiments

The mouse models of CRC liver metastasis were injected intraperitoneally with different doses of NE (TCI, China). Eighteen SPF-grade male BALB/c mice aged 8 weeks were randomly divided into three groups 3

days after successful modeling: a) control group, injected with normal saline; b) low-dose NE group, injected with 0.28 nmol NE; and c) high-dose NE group: injected with 2.8 nmol NE. NE was prepared with 0.9% saline and stored in a refrigerator at -20℃. NE was prepared every 3 days and injected intraperitoneally every 2 days (0.1 ml) for a total of 8 sessions.

Immunohistochemistry

Mouse liver tissue was collected, paraffin-embedded, and sliced into 4-μm-thick sections. After dewaxing, hydration, antigen repair, and incubation with 3% H_2O_2 solution in the dark at room temperature, rabbit anti-mouse primary anti-F4/80 monoclonal antibody (1:500, Servicebio, China) was added, and color development was performed using a DAB staining immunohistochemistry kit (Zsbio, China). Under microscope, three high-magnification fields were randomly selected for image acquisition, and the positive areas were analyzed using the Image J software.

Cell culture

Both the murine colon carcinoma cell line CT-26 (Cell Bank of Chinese Academy of Sciences, China) and the KCs (Jennio Biotech, Guangdong, China) were cultured in RPMI 1640 medium supplemented with 10% fetal bovine serum (FBS) and 1% penicillin/streptomycin (100 U/mland 100 μg/ml, respectively) at 37°C with 5% CO_2 in a thermostat incubator.

Enzyme-linked immunosorbent assay (ELISA)

All the ELISA kits were purchased from Arigo, USA. After blocking, antibodies TGF-β, IL-6, and VEGF were added for inoculation. After the enzyme reaction was terminated, the optical density (OD) of each well was measured at 450 nm.

Flow cytometry

After KCs were inoculated at a density of $1{\cdot}10^5$ cells/well in 6-well plates for 24 h, 100 μl PBS as well as 10^{-9} M, 10^{-8} M, 10^{-7} M, 10^{-6} M, and 10^{-5} M NE were added for another 24 h inoculation. After KCs were inoculated at a density of $1{\cdot}10^5$ cells/well in 6-well plates for 24 h, 100 μl PBS and 10^{-9} M, 10^{-8} M, 10^{-7} M, 10^{-6} M, and 10^{-5} M ICI118551 were added for pre-treatment, followed by addition of 10^{-9} M NE for another 24 h incubation. After KCs were inoculated at a density of $1{\cdot}10^5$ cells/well in 6-well plates for 24 h, 100 μl PBS and 10, 20 and 40 μmol/L LY294002 were added for pre-treatment, followed by addition of 10^{-9} M NE for another 24 h incubation. Subsequently, 10 μl FITC-CD86 antibody or PE-CD206 antibody (BD, America) was added to each group separately, and the results were detected using a flow cytometer (Eplcs XL model, Beckman Coulter, Inc, USA).

Transwell migration assay

KCs were inoculated in 24-well plates at a density of $2{\cdot}10^5$cells/500 μl in the lower chamber for 24 h. The lower chamber was added with 50 μl PBS as well 10^{-9} M, 10^{-8} M, 10^{-7} M, 10^{-6} M, and 10^{-5} M NE for 24 h inoculation. Alternately, 50 μl PBS as well as 10^{-9} M, 10^{-8} M, 10^{-7} M, 10^{-6} M, 10^{-5} M ICI118551 were

added for 2 h pre-treatment, followed by addition of 50 μl 10^{-9} M NE for another 24 h inoculation. Subsequently, the culture medium was replaced with 500 μl RPMI-1640 medium containing 20% FBS. CT26 cell suspension free of FBS was inoculated at a concentration of $4{\cdot}10^4$ cells/100 μl in the upper chamber and co-inoculated with the pre-treated KCs for 24 h. The cells were fixed in 4% paraformaldehyde solution for 30 min and stained with 0.1% crystalline violet for 20 min. Three fields viewed at 200X were randomly selected for each group. The number of cells crossing the microporous membrane in the upper chamber was counted using the Image J software.

Bioinformatics analysis

The GSE81980 dataset (100 non-hepatic metastases and 50 liver metastases samples) and the GSE18105 dataset (67 non-hepatic metastases and 44 liver metastases samples) in the Gene Expression Omnibus (GEO, http://www.ncbi.nlm.nih.gov/geo) were searched for genes associated with CRC liver metastases. We compared two samples from the two datasets at the GEO2R platform (http://www.ncbi.nlm.nih.gov/geo/geo2r). With the help of the FunRich software, 11 common differential genes of each dataset were identified: *HNRNPC, MROH1, MAPK1, AKT2, F5, SCAMP1, ANKFN1, GFM1, ABHD12, PLCG2,and MARVELD3*. A protein-protein interaction (PPI) network was constructed using the STRING website (http://string-db.or, Version 11.0). Using *P*□0.01 as the screening condition, 23 differential genes were identified: PLRG1, CWC15, PEA15, EFTUD2, PPP2CA, U2AF2, RPS6KA1, DDX RPS6KA1, DDX39B, HNRNPC, MAPK1, PPP2R1A, AKT2, HNRNPA2B1, HNRNPA1, PDPK1, HNRNPL, HNRNPM, PRPF19, BCAS2, CDC5L, SNRNP200, THOC2, and ALYREF. Gene ontology and KEGG enrichment analyses were performed at the DAIVD website (https://david-d.ncifcrf.gov/home.jsp, Version 6.8).

TISIDB (http://cis.hku.hk/TISIDB/) enables the analysis of the associations of a selected gene with the clinical features of tumors, immunomodulators and chemokines. In order to understand whether chemokines are correlated with macrophages, we analyzed the chemokines including CXCL12, CXCL9, CCL2, CCL20, CXCL8, CXCL16, CX3CL1, and CCL17 in CRC through the TISIDB website.

Western blotting

Protein samples were separated by SDS-polyacrylamide gel electrophoresis, transferred to nitrocellulose, and incubated with monoclonal rabbit anti-mouse anti-PI3K (1:2000, ABclonal, China), anti-total-Akt (PAN-Akt, 1:1000, ABclonal, China), anti-phosphorylated-Akt (p-Akt, 1 :1000, ABclonal, China), anti-α_2-AR (1:500, GeneTex, USA), anti-β_2-AR (1:1000, Abcam, USA) primary antibodies overnight at 4°C. After adding secondary antibodies and chromogenic reagents, the bands were visualized using the ChemiDoc XRS system (Bio-Rad Laboratories) and gray-scale value was quantified with Quantity One (Bio-Rad Laboratories). With β-actin as an internal reference, the relative expression levels of PI3K, PAN-Akt, p-Akt were calculated.

Quantitative reverse transcription PCR (RT-qPCR)

KCs were treated with PBS and 10^{-9} M NE for 24 h, and then the total RNA was extracted using TRIzol reagent (Invitrogen, USA). cDNA reverse transcription was performed using PrimeScript™ RT reagent kit. The obtained data were analyzed by the $2^{-\Delta\Delta CT}$ method. The primer sequences of CXCL12, CXCL9, CCL2, CCL20, CXCL8, CXCL16, CX3CL1, and CCL17 are shown in Table 1.

Table 1
The primer sequences of the targeted genes

Item	Primer sequence (5'-3')	Product size (bp)
CXCL12 Forward primer	TCAATGCCTGAAGACCCTGC-X2	188
Reverse primer	GCCTTCGGTTTGTTVAGTATCT	
CXCL9 Forward primer	GCATCAGCACCAGCCGA-X2	275
Reverse primer	CCTTGAACGACGACGACTTTG	
CCL2 Forward primer	GCTGACCCCAAGAAGGAATG-X4	183
Reverse primer	TGAGGTGGTTGTGGAAAAGG	
CCL20 Forward primer	CAGCCAGGCAGAAGCAGCAA-XA2	102
Reverse primer	GGCCATCTGTCTTGTGAAACCCA	
CXCL8 Forward primer	CTCCTGCTGGCTGTCCTTA	167
Reverse primer	GCTATCACTTCCTTTCTGTTGC	
CXCL16 Forward primer	CACTTTACAAACCAGCAGAC	153
Reverse primer	AGTTTGAGAAGCGGGTGGAC	
CX3CL1 Forward primer	AGTTTGAGAAGCGGGTGGAC	217
Reverse primer	TCCTGTGCCTCGGAAGTTGA	
CCL17 Forward primer	CCGCTGAGGCATTTGGAGAC	178
Reverse primer	TGAGGGAGGAAGGCTTTATT	
β-actin Forward primer	CGTTGACATCCGTAAAGACCTC	159
Reverse primer	ACAGAGTACTTGCACTCAGGAG	

Statistical analysis

Statistical analysis was performed using the SPSS 21.0. The count data are presented as numerical values and percentages and compared with Chi-square test. A *P* value <0.05 was considered significantly different.

Results

NE promoted CRC liver metastasis and reduced intrahepatic KC content

Mouse models of CRC liver metastasis were established by injection of CT26 cells via splenic vein, and different doses of NE were injected intraperitoneally. The number of liver metastases in the control, low-dose (0.28 nmol) NE, and high-dose (2.8 nmol) NE groups were 33.4±20.9, 111.00±51.43, and 102.40±54.85, respectively, and NE promoted the occurrence of liver metastases at either low or high doses (both $P<0.05$) (Fig. 1A-B). To observe the effect of NE on KCs, we performed immunohistochemical staining using F4/80 as a marker of KC cells. It was found that KCs were mainly distributed in the hepatic sinusoids and the central vein or confluent regions of the hepatic lobules, and the distribution of KCs in both the low- and high-dose NE groups was less than that in the control group (both $P < 0.05$), while there was no statistical difference between the two NE groups (Fig. 1C).

NE induced the M2 polarization of KCs

After 24 h incubation, KCs were treated with gradient concentrations of NE. The polarization status of KCs was measured at 24 h (A CD86 marker for M1 and a CD206 marker for M2). The results showed that all concentrations of NE inhibited CD86 expression on the surface of KCs ($P < 0.01$). In addition, low to medium concentrations of NE (10^{-9} M, 10^{-8} M, and 10^{-7} M) promoted CD206 expression on the surface of KCs ($P < 0.01$). However, when the concentrations increased to 10^{-6} M and 10^{-5} M, NE had no effect on CD206 expression on the surface of KCs (Fig. 2A-B).

Furthermore, we examined the effect of NE on KC-secreted cytokines by ELISA. The results showed that each concentration of NE inhibited the secretion of IL-6 by KC in a dose-dependent manner ($P < 0.01$). While low concentrations (10^{-9} M and 10^{-8} M) of NE promoted the secretion of VEGF and TGF-β by KC ($P < 0.01$), higher concentrations (10-7 M, 10-6 M, and 10-5 M) of NE showed no effect on the secretion of VEGF and TGF-β (Fig. 2C). Therefore, low-concentration NE could induce the M2 polarization of KCs.

NE induced KC polarization via β_2-AR on the surface of KCs

To identify the specific receptor via which NE exerts an effect on KC polarization, we selected the lowest concentration (10^{-9} M) of NE in the above experiment to treat KC firstly and then detected the expressions

of α_2-AR and β2-A_2 on the surface of KCs after 24 h. The results showed that low-concentration NE induced up-regulation of β2-AR expression in KCs but had no effect on α_2-AR expression (Fig. 3A), suggesting that NE may exert its effect via the β2-AR on the surface of KCs.

KCs were further pretreated with gradient concentrations ((10^{-9} M, 10^{-8} M, 10^{-7} M, 10^{-6} M, and 10^{-5} M) of a β_2-AR blocker ICI118551, and an equal concentration of NE (10^{-9} M) was added 2 h later before incubation for 24 h. It was found that the expression level of CD206 on KC decreased after the addition of a β_2-AR blocker compared to the control group, and there were statistical differences ($P < 0.05$) when the concentrations reached 10^{-6} M and 10^{-5} M (Fig. 3C).

ELISA revealed that the secretion of IL-6 showed an increasing trend after treatment of KC with gradient concentrations of the β_2-AR blocker ICI118551, and the difference was statistically significant ($P < 0.01$) at the concentrations of 10^{-5} M. Although no statistical difference was observed, KCs treated with the β2-AR blocker showed a decreasing trend in the secretion of cytokines VEGF and TGF-β (Fig. 3B). Therefore, NE might promote the M2 polarization of KCs via β_2-AR on the surface of KCs.

NE affected KC polarization and function by activating PI3K/Akt pathway

Differential genes were screened by comparing genes from CRC non-liver metastasis samples and liver metastasis samples in datasets GSE81980 and GSE18105. The obtained differential genes underwent further functional and pathway enrichment analyses using the DAVID website. It was found that GO categories were enriched in cellular component, biological process, molecular function, serine/threonine protein kinases, serine phosphorylation, threonine phosphorylation, and DNA damage checkpoint signaling. The KEGG analysis revealed that the most significant enrichment pathways were PI3K-Akt signaling pathway, sphingolipid signalling pathway, β-Adrenergic signaling in cardiomyocytes, and neurotrophin signaling pathway (Fig. 4. A).

To verify that NE promotes KC M2 polarization through PI3K/Akt signaling, we treated KCs with PBS in the control group and gradient concentrations of NE in the NE groups and detected the expressions of PI3K, PAN-Akt, and p-Akt proteins in KCs by Western blotting after 24 h. The results showed that low concentrations (10^{-9} M and 10^{-8} M) of NE induced an increase in PI3K protein expression compared to the control group ($P < 0.01$). In addition, the expressions of PAN-Akt and p-Akt proteins in KCs also increased in the low-concentration (10^{-9} M) NE group ($P < 0.05$) (Fig. 4B).

All the gradient concentrations of the β_2-AR receptor blocker inhibited the expressions of PI3K, Akt and p-Akt proteins on KCs (Fig. 4C). Thus, NE might promote high expressions of PI3K, PAN-Akt, and p-Akt proteins in KCs by acting on β_2-AR. We further applied the PI3K inhibitor LY294002 to block the PI3K/Akt signaling pathway and then gave NE treatment; it was found that the expression of CD206 on the surface of KCs decreased, and the amounts of VEGF and TGF-β secreted by LY294002-treated KCs showed a

decreasing trend, and the difference was statistically significant when the concentration was 40 μmol/L ($P < 0.01$); IL- 6 showed an increasing trend but did not yet reach statistical difference. (Fig. 4) It could be concluded that NE/β2-AR promoted KC M2 polarization through the PI3K/Akt pathway.

M2 KC promoted the directional migration of CT26 cells via CXCL12

After 24 h incubation, KCs were treated with gradient concentrations of NE. The effect of M2 KC on the migration of colon cancer cells was observed using Transwell assay. The results showed that M2 KC treated by low concentration of NE promoted the migration of CT26 cells compared with the control group ($P < 0.01$). (Fig. 5A)

KCs were further pretreated with gradient concentrations ((10^{-9} M, 10^{-8} M, 10^{-7} M, 10^{-6} M, and 10^{-5} M) of a β_2-AR blocker ICI118551, and an equal concentration of NE (10^{-9} M) was added 2 h later before incubation for 24 h. Transwell migration assay suggested that KC treated with high concentrations (10-6 M, 10-5 M) of ICI118551 had a significantly reduced pro-migration effect on CT26 cells ($P < 0.01$) (Fig. 5B). Thus, low concentrations of the enteroneurotransmitter NE/β2-AR induced intrahepatic KC M2 polarization and the M2 KCs promoted the migration of CT26 cells.

Eight macrophage-assocaited chemokines were screened from the TISIDB website. As verified by RT-PCR, the expression of CXCL12 in KCs induced by low concentration (10^{-9} M) of NE was significantly higher than that in the control group (P=0.006), while the expressions of CXCL9, CCL2, CCL20, CXCL8, CXCL16, CX3CL1, and CCL17 were significantly lower than those in the control group (all P<0.05) (Fig. 5C-D). CXCL12 expression in KCs was detected using the RT-PCR, which showed that high concentrations (10^{-6} M and 10^{-5} M) of the β2-AR blocker significantly down-regulated CXCL12 expression in KCs ($P < 0.05$) (Fig. 5E). Therefore, M2 KC might promote the directional migration of CT26 cells by upregulating CXCL12 expression.

Discussion

In the present study, we found that low-concentration NE/β2-AR could promote intrahepatic colorectal metastases by inducing the M2 polarization of Kupffer cells (KC) and upregulating the CXCL12 expression on KC. Our findings are of great significance for elucidating the mechanism of colorectal cancer liver metastasis and developing strategies to prevent and treat liver metastasis.

We found for the first time that in animal models, NE promoted colorectal liver metastases, which was consistent with the literature. Palm *et al.* reported that tumor progression was significantly accelerated after intraperitoneal injection of NE in prostate cancer-bearing mice.[20] Similarly, NE also promoted the progression of colorectal cancer. Han *et al.* incubated colon cancer cells (HCT-116) with NE at a concentration of 10^{-7} M for 24 h and found that NE promoted the proliferation, invasion, and migration of colon cancer cells; and NE promoted colorectal cancer progression by activating the CREB1-miR-373 axis.

[21] Several studies have demonstrated that stress-induced activation of the adrenergic system not only promotes the proliferation of cancer cells themselves but also contributes to the metastasis of malignant tumours.[21, 22] It has been shown that NE promotes the migration of colon cancer cells by binding to the β2-AR on tumor surface, while propranolol, a β-blocker, prevents the liver metastasis of colon cancer.[23, 24]

In fact, enteric neurotransmitters are also involved in the remodeling of liver immunity.[25] Recent studies have shown that the microenvironment of colorectal cancer intrahepatic metastasis is rich in immunosuppressive cells (e.g. MRC1+ CCL18+ M2-like macrophages) derived from intrahepatic KC.[26] The present study confirmed that NE not only reduced intrahepatic KC content but also promoted KC M2 polarization, leading to an immunosuppressive microenvironment in the liver, which facilitated the metastatic colonization of cancer cells into the liver. As liver resident macrophages, KCs form the first-line defense against pathogens passing through the portal circulation, playing a key role in regulating liver immunity.[27] It has been found that tumor cells can form pre-metastatic niches by releasing exosomes to induce the M2 polarization of KC.[28] A meta-analysis showed that the rate of liver metastasis from colorectal cancer was significantly lower in rats with cirrhosis.[29] Liver KC in rats with cirrhosis secretes cytokines that induce upregulation of Fas receptor protein expression on colorectal cancer cells andpromote cancer cell binding to FasL on intrahepatic cytotoxic T lymphocytes, thereby killing cancer cells.[30] In addition, KC secretes cytokines (e.g. VEGF) and matrix metalloproteinases, which accelerate tumor cell invasion into the liver and promote tumor proliferation and angiogenesis, enhancing colorectal cancer liver metastasis.[31] However, some studies have also shown that colorectal cancer liver metastasis is associated with NE-induced activation of NK cells in the tumor microenvironment.[32] Therefore, the effect of NE on intrahepatic immune status may be multifaceted.

We further found that NE was induced by β2-AR on the surface of KC to polarize KC towards the M2 type. Interestingly, we noted that the effect of NE on KC polarization was closely related with dose, showing bidirectional regulation. The known M1-type and M2-type KCs are not completely opposing, but rather they can be interconverted. Huan *et al.* found that the sympathetic nervous system could promote KC activation and maintain the inflammatory microenvironment in the liver by activating α-AR on KCs, ultimately accelerating the progression of hepatocellular carcinoma.[33] In contrast, Loegering *et al.* found that catecholamines could inhibit the clearance function of KCs via β-AR on KCs.[34] Our results showed that low-concentration NE promoted KC polarization towards the M2 phenotype, whereas high-concentration NE promoted KC conversion to the M1 phenotype, which may be related to the different receptors on which they act. Other studies have shown that low-concentration NE (10^{-9} to 10^{-7}M) bind mainly to α_2-AR to exert the pro-inflammatory effects, whereas high-concentration NE (10^{-7} to 10^{-5}M) bind to β_2-AR to exert the anti-inflammatory effects.[35] NE exerted its anti-inflammatory effects by inhibiting KC polarization towards pro-inflammatory M1 phenotype via β_2-AR and by down-regulating the expressions of perforin, granzyme B and IFN-γ[36], and the NE-induced liver injury was associated with its up-regulation of α_2-AR in intrahepatic KCs, which caused TNF-α release[37]. In our experiment, we further determined the expressions of β_2-AR and α_2-AR on the surface of NE-treated KCs and found that NE-

induced expression of β_2-AR on KCs was significantly higher than in the control group, while there was no significant change in the expression of α_2-AR. When a β_2-AR receptor blocker was added, the markers of M2-type KC were down-regulated, which in turn affected the migration of CT26. Our results showed that NE binded to the β_2-AR on the surface of KCs and promoted its M2 polarization, ultimately affecting the migration of colon cancer cells. The mechanism may be related to the reduced secretion of TNF-α and NF-κB due to impaired cholesterol metabolism in adipose tissue.[38] The activation of the phosphatidylinositol 3-kinase (PI3K) pathway may be another possible mechanism. It has been reported that the tumor-secreted metastasis-associated secretory protein histone K can stimulate the M2 polarization of TAM via the PI3K/Akt pathway.[39, 40]

By analyzing the differential genes in colorectal cancer non-liver metastasis and colorectal cancer liver metastasis samples, we found that PI3K/Akt pathway played an important role in colorectal cancer liver metastasis. Our results also revealed that the expressions of PI3K, PAN-Akt and p-Akt proteins on KCs were significantly higher in NE induction group than in the control group, while the expressions of these proteins decreased significantly after β_2-AR inhibition. Further inhibition of the PI3K/Akt pathway down-regulated the expression of CD206 on KCs, suggesting that NE binds to β_2-AR on KCs and induces KC M2 polarization by activating the PI3K/Akt pathway. Kim *et al*. found that fucoxanthin (FCX), a xanthophyll carotenoid, could inhibit LPS-induced macrophage polarization and reduce the secretion of IL-6, TNF-α and IL-1β by activating the PI3K/Akt pathway, thus promoting the infiltration of tumor cells.[41] Wang *et al*. showed that green tea polyphenols could inhibit the expressions of CXCL12 and VEGF in tumor cells through PI3K/Akt/mTOR/hypoxia inducible factor-1αpathway, thereby resisting tumor angiogenesis.[42] However, the mechanism by which NE affects the directional migration of colorectal cancer cells is still unclear. Our results suggested that KCs treated with low-concentration (10^{-9} M) NE significantly induced the migration of CT26 cells, suggesting that M2 KC has a role in promoting CT26 migration.

Cancer cell homing has been reported to be influenced by the binding of chemokine receptors in cancer cells to specific ligands in target organs.[43] During tumor metastasis, CXCL12 can activate its receptor CXCR4 in a paracrine or autocrine manner to initiate the early-stage - metastasis; when tumor cells enter the circulation, CXCR4-positive tumor cells tend to migrate to target organs with high CXCL12 expression, such as the liver, lungs, and lymph nodes; after these cells settle in the target organs, the CXCL12/CXCR4 axis may provide further support for their growth.[44, 45] M2 macrophages or TAMs can secrete chemokines such as CXCL8, CXCL12, and CCL2 to promote the proliferation of lung cancer cells.[46] In addition, M2 macrophages promote CXC ligand expression, which is associated with high infiltration of CRC. CXCL12 can promote distant metastasis of colorectal cancer by upregulating Homeobox B5 (HOXB5), a member of the HOX transcriptional factor family, to activate CXCR4.[47, 48] The activation of the CXCL12-CXCR4 axis initiates not only CXCR4-positive tumor cells but also CXCR4-positive bone marrow-derived dendritic cells, which promote angiogenesis in a VEGF-dependent manner and are involved in tumor metastasis.[49, 50] In addition, CXCL12 in the tumor microenvironment can promote colon cancer migration by activating the PI3K/Akt pathway via binding to CXCR4 on colon cancer cells;

the CXCL12-CXCR4 axis can activate the PI3K/Akt pathway to promote craniopharyngeal carcinoma migration; and CXCL12 signaling can also induce epithelial-mesenchymal transition of glioblasts through the PI3K/Akt pathway to promote glioblastoma migration.[51–53] Our results suggested that M2 KCs might induce the directional migration of CT26 cells via CXCL12 and might further activate the PI3K/Akt pathway to induce the M2 polarization of KCs.

There are some limitations in the present study: a) only one cell line (CT26) was used; and b) the findings were not validated in *in vivo* experiments.

In conclusion, the effect of NE as an enteric neurotransmitter on colorectal cancer liver metastasis may be related to the polarization of intrahepatic KCs. Low-concentration NE/β_2-AR may induce intrahepatic KC M2 polarization through the PI3K/Akt pathway and promote its secretion of CXCL12 to induce colorectal cancer liver metastasis.

Declarations

Ethics approval and consent to participate

This study was approved by the Administration Committee of Experimental Animals, Hebei General Hospital, Hebei Province, China. All of the experimental animal procedures were conducted in accordance with the requirements of the Regulations of Hebei Medical University on the Management and Use of Experimental Animals (License: SYXK (Hebei) 2015-0065).

Consent for publication

Not applicable

Availability of data and materials

The datasets generated and/or analyzed during the current study are available from the corresponding author.

Competing interests

The authors declare that they have no competing interests.

Funding

This work was supported by the Program of Clinical Excellent Talents of Hebei Province (Grant No. 81172332).

Authors' contributions

Xiaoyan Li, Na Yuan, Ce Zhou and Jie Zhi : Performed the experiments;

Yang Li, Bin Wang and Wujie Zhao: Analyzed the data;

Yitao Jia : Designed the experiments and prepared the manuscript and submitted the final manuscript.

Acknowledgements

The authors wish to express their sincere thanks to all those who have helped during the course of writing this paper. We thank Dr Jia, the Third Department of Oncology of Hebei General Hospital, for conceiving and designing the study.

The study was carried out in compliance with the ARRIVE guidelines

References

1. Sung H, Ferlay J, Siegel RL, et al. Global cancer statistics 2020: GLOBOCAN estimates of incidence and mortality worldwide for 36 cancers in 185 countries. CA Cancer J Clin. 2021;71(3):209–249.
2. Lim CJ, Lee YH, Pan L, et al. Multidimensional analyses reveal distinct immune microenvironment in hepatitis B virus-related hepatocellular carcinoma. Gut. 2019; 68(5): 916–927.
3. Konopke R, Roth J, Volk A, et al. Colorectal liver metastases: an update on palliative treatment options. J Gastrointestin Liver Dis. 2012;21(1): 83–91.
4. Imai K, Allard MA, Benitez CC, et al. Early Recurrence After Hepatectomy for Colorectal Liver Metastases: What Optimal Definition and What Predictive Factors. Oncologist. 2016;21(7): 887–894.
5. Jia B. Commentary: Gut microbiome-mediated bile acid metabolism regulates liver cancer via NKT cells. Front Immunol. 2019;10: 282.
6. Dai S, Liu F, Qin Z, et al. Kupffer cells promote T-cell hepatitis by producing CXCL10 and limiting liver sinusoidal endothelial cell permeability. Theranostics. 2020;10(16): 7163–7177.
7. Li H, Zhou Y, Wang H, et al. Crosstalk Between Liver Macrophages and Surrounding Cells in Nonalcoholic Steatohepatitis. Front Immunol. 2020;11: 1169.
8. Yang L, Li T, Shi H, et al. The cellular and molecular components involved in pre-metastatic niche formation in colorectal cancer liver metastasis. Expert Rev Gastroenterol Hepatol. 2021;15(4): 389–399.
9. Hassan R. Kupffer cells in hepatotoxicity. Excli J. 2020;19:1156–1157.
10. Ye YC, Zhao JL, Lu YT, et al. NOTCH signaling via WNT regulates the proliferation of alternative, CCR2-independent tumor-associated macrophages in hepatocellular carcinoma. Cancer Res. 2019;79(16):4160–4172.
11. Miyake Y, Yamamoto K. Role of gut microbiota in liver diseases. Hepatol Res. 2013;43(2):139–146.
12. Ma C, Han M, Heinrich B, et al. Gut microbiome-mediated bile acid metabolism regulates liver cancer via NKT cells. Science. 2018;360(6391).

13. Jansen L, Hoffmeister M, Arndt V, et al. Stage-specific associations between beta blocker use and prognosis after colorectal cancer. Cancer. 2014;120(8): 1178–1186.
14. Haldar R, Ricon-Becker I, Radin A, et al. Perioperative COX2 and β-adrenergic blockade improves biomarkers of tumor metastasis, immunity, and inflammation in colorectal cancer: A randomized controlled trial. Cancer. 2020;126(17): 3991–4001.
15. Ahl R, Matthiessen P, Fang X, et al. Effect of beta-blocker therapy on early mortality after emergency colonic cancer surgery. Br J Surg. 2019;106(4): 477–483.
16. Chen M, Qiao G, Hylander BL, et al. Adrenergic stress constrains the development of anti-tumor immunity and abscopal responses following local radiation. Nat Commun. 2020;11(1):1821.
17. Daher C, Vimeux L, Stoeva R, et al. Blockade of β-Adrenergic receptors improves CD8+ T-cell priming and cancer vaccine efficacy. Cancer Immunol Res. 2019;7(11):1849–1863.
18. Sun Z, Hou D, Liu S, et al. Norepinephrine inhibits the cytotoxicity of NK92MI cells via the β2adrenoceptor/cAMP/PKA/pCREB signaling pathway. Mol Med Rep. 2018;17(6):8530–8535.
19. Mohammadpour H, MacDonald CR, Qiao G, et al. β2 adrenergic receptor-mediated signaling regulates the immunosuppressive potential of myeloid-derived suppressor cells. J Clin Invest. 2019;129(12):5537–5552.
20. Palm D, Lang K, Niggemann B, et al. The norepinephrine-driven metastasis development of PC-3 human prostate cancer cells in BALB/c nude mice is inhibited by beta-blockers. Int J Cancer. 2006;118(11): 2744–2749.
21. Han J, Jiang Q, Ma R, et al. Norepinephrine-CREB1-miR-373 axis promotes progression of colon cancer. Mol Oncol. 2020;14(5):1059–1073.
22. Zhang H, Miao J, Li F, et al. Norepinephrine transporter promotes the invasion of human colon cancer cells. Oncol Lett. 2020;19(1): 824–832.
23. Masur K, Niggemann B, Zanker KS, et al. Norepinephrine-induced migration of SW 480 colon carcinoma cells is inhibited by beta-blockers. Cancer Res. 2001;61(7): 2866–2869.
24. Sorski L, Melamed R, Matzner P, et al. Reducing liver metastases of colon cancer in the context of extensive and minor surgeries through β-adrenoceptors blockade and COX2 inhibition. Brain Behav Immun. 2016;58: 91–98.
25. Clarke TB, Davis KM, Lysenko ES, et al. Recognition of peptidoglycan from the microbiota by Nod1 enhances systemic innate immunity. Nat Med. 2010;16(2): 228–231.
26. Wu Y, Yang S, Ma J, et al. Spatiotemporal Immune Landscape of Colorectal Cancer Liver Metastasis at Single-Cell Level. Cancer Discov. 2021; DOI: 10.1158/2159-8290.CD-21-0316.
27. Wang L, Sun Y, Yi M, et al. IEO model: A novel concept describing the complete metastatic process in the liver microenvironment. Oncol Lett. 2020;19(6):3627–3633.
28. Zhao S, Mi Y, Guan B, et al. Tumor-derived exosomal miR-934 induces macrophage M2 polarization to promote liver metastasis of colorectal cancer. J Hematol Oncol. 2020;13(1):156.

29. Cai B, Liao K, Song XQ, et al. Patients with chronically diseased livers have lower incidence of colorectal liver metastases: a meta-analysis. PLoS One. 2014;9(9):e108618.
30. Song E, Chen J, Ouyang N, et al. Kupffer cells of cirrhotic rat livers sensitize colon cancer cells to Fas-mediated apoptosis. Br J Cancer. 2001;84(9):1265–1271.
31. Li M, Lai X, Zhao Y, et al. Loss of NDRG2 in liver microenvironment inhibits cancer liver metastasis by regulating tumor associate macrophages polarization. Cell Death Dis. 2018;9(2):248.
32. Sorski L, Melamed R, Matzner P, et al. Reducing liver metastases of colon cancer in the context of extensive and minor surgeries through β-adrenoceptors blockade and COX2 inhibition. Brain Behav Immun. 2016;58: 91–98.
33. Huan HB, Wen XD, Chen XJ, et al. Sympathetic nervous system promotes hepatocarcinogenesis by modulating inflammation through activation of alpha1-adrenergic receptors of Kupffer cells. Brain Behav Immun. 2017;59:118–134.
34. Loegering DJ, Commins LM. Effect of beta-receptor stimulation on Kupffer cell complement receptor clearance function. Circ Shock. 1988;25(4):325–332.
35. Brinkman DJ, Ten Hove AS, Vervoordeldonk MJ, et al. Neuroimmune interactions in the gut and their significance for intestinal immunity. Cells. 2019;8(7).
36. Bacou E, Haurogné K, Allard M, et al. β2-adrenoreceptor stimulation dampens the LPS-induced M1 polarization in pig macrophages. Dev Comp Immunol. 2017;76: 169–176.
37. Ajakaiye MA, Jacob A, Wu R, et al. Upregulation of Kupffer cell α2A-Adrenoceptors and downregulation of MKP-1 mediate hepatic injury in chronic alcohol exposure. Biochem Biophys Res Commun. 2011; 409(3): 406–411.
38. Huang JP, Hsu SC, Meir YJ, et al. Role of dysfunctional adipocytes in cholesterol-induced nonobese metabolic syndrome. J Mol Endocrinol. 2018;60(4): 307–321.
39. Li R, Zhou R, Wang H, et al. Gut microbiota-stimulated cathepsin K secretion mediates TLR4-dependent M2 macrophage polarization and promotes tumor metastasis in colorectal cancer. Cell Death Differ. 2019;26(11): 2447–2463.
40. Grailer JJ, Haggadone MD, Sarma JV, et al. Induction of M2 regulatory macrophages through the β2-adrenergic receptor with protection during endotoxemia and acute lung injury. J Innate Immun. 2014;6(5): 607–618.
41. Kim M, Kang H, Li Y, et al. Fucoxanthin inhibits lipopolysaccharide-induced inflammation and oxidative stress by activating nuclear factor E2-related factor 2 via the phosphatidylinositol 3-kinase/AKT pathway in macrophages. Eur J Nutr. 2021.
42. Wang J, Man G, Chan TH, et al. A prodrug of green tea polyphenol (-)-epigallocatechin-3-gallate (Pro-EGCG) serves as a novel angiogenesis inhibitor in endometrial cancer. Cancer Lett. 2018;412:10–20.
43. Itatani Y, Kawada K, Inamoto S, et al. The role of chemokines in promoting colorectal cancer Invasion/metastasis. Int J Mol Sci. 2016;17(5).

44. Jung Y, Kim JK, Shiozawa Y, et al. Recruitment of mesenchymal stem cells into prostate tumours promotes metastasis. Nat Commun. 2013;4:1795.
45. López-Gil JC, Martin-Hijano L, Hermann PC, et al. The CXCL12 crossroads in cancer stem cells and their niche. Cancers (Basel). 2021;13(3).
46. Zhou Y, Li J, Han B, et al. Schwann cells promote lung cancer proliferation by promoting the M2 polarization of macrophages. Cell Immunol. 2020;357:104211.
47. Wu Y, Yuan L, Lu Q, et al. Distinctive profiles of tumor-infiltrating immune cells and association with intensity of infiltration in colorectal cancer. Oncol Lett. 2018;15(3):3876–3882.
48. Feng W, Huang W, Chen J, et al. CXCL12-mediated HOXB5 overexpression facilitates colorectal cancer metastasis through transactivating CXCR4 and ITGB3. Theranostics. 2021;11(6):2612–2633.
49. Du R, Lu KV, Petritsch C, et al. HIF1alpha induces the recruitment of bone marrow-derived vascular modulatory cells to regulate tumor angiogenesis and invasion. Cancer Cell. 2008;13(3): 206–220.
50. Hiratsuka S, Duda DG, Huang Y, et al. C-X-C receptor type 4 promotes metastasis by activating p38 mitogen-activated protein kinase in myeloid differentiation antigen (Gr-1)-positive cells. Proc Natl Acad Sci U S A. 2011;108(1): 302–307.
51. Ma J, Sun X, Wang Y, et al. Fibroblast-derived CXCL12 regulates PTEN expression and is associated with the proliferation and invasion of colon cancer cells via PI3k/Akt signaling. Cell Commun Signal. 2019, 17(1):119.
52. Yin X, Liu Z, Zhu P, et al. CXCL12/CXCR4 promotes proliferation, migration, and invasion of adamantinomatous craniopharyngiomas via PI3K/AKT signal pathway. J Cell Biochem. 2019;120(6):9724–9736.
53. Lv B, Yang X, Lv S, et al. CXCR4 Signaling Induced Epithelial-Mesenchymal Transition by PI3K/AKT and ERK Pathways in Glioblastoma. Mol Neurobiol. 2015;52(3):1263–1268.

Figures

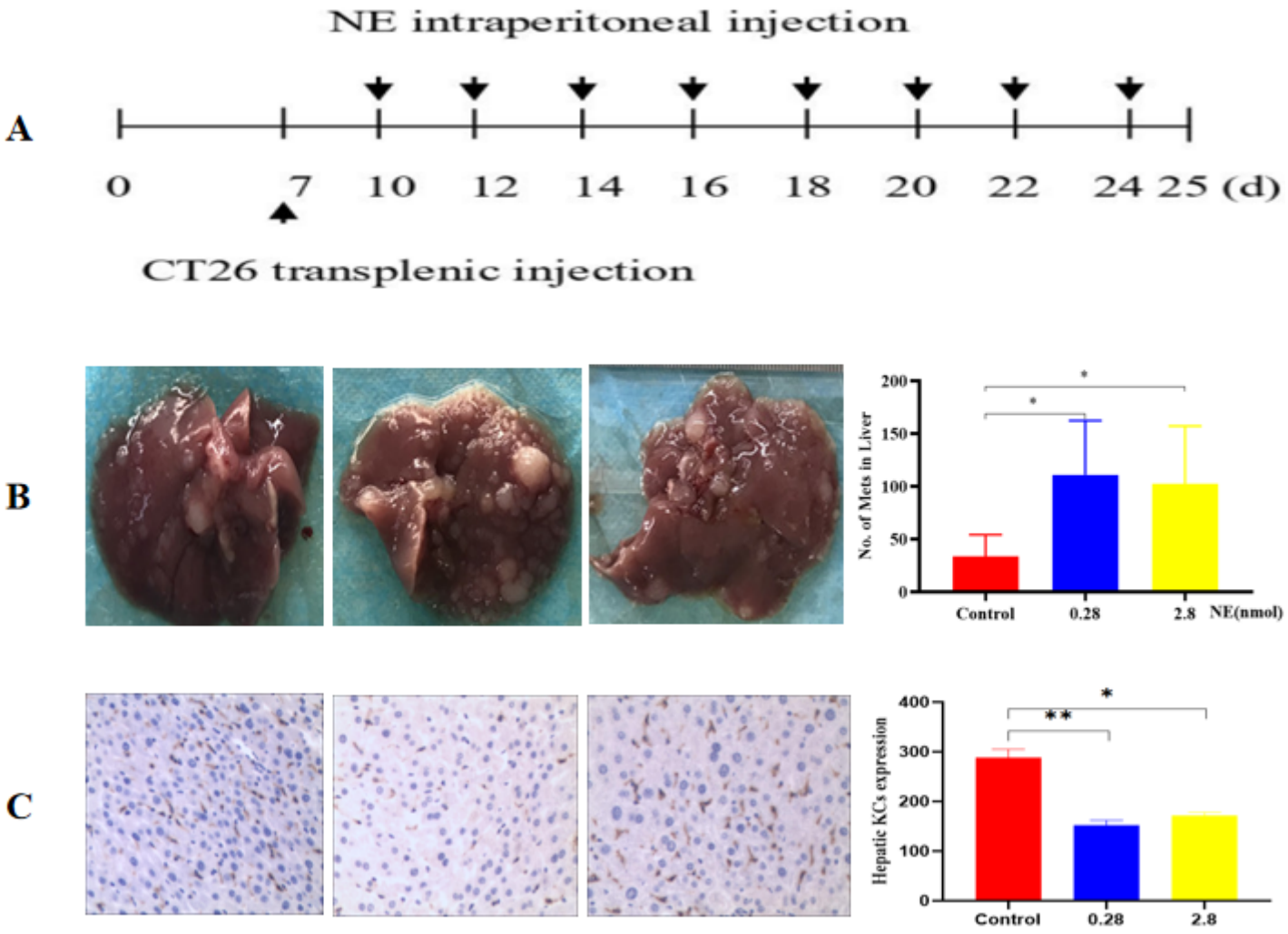

Figure 1

NE promoted CRC liver metastasis and reduced intrahepatic KC content. **A**) Schematic diagram of the experiment (upper arrow: NE was injected intraperitoneally at 0.1 ml every 2 days for 8 sessions; lower arrow: CT26 cells were injected via splenic vein to establish a CRC liver metastasis model); **B**) images and numbers of CRC liver metastases in the control, low-dose NE, and high-dose NE groups (n=6); **C**) images and numbers of KCs in the control, low-dose NE, and high-dose NE groups.

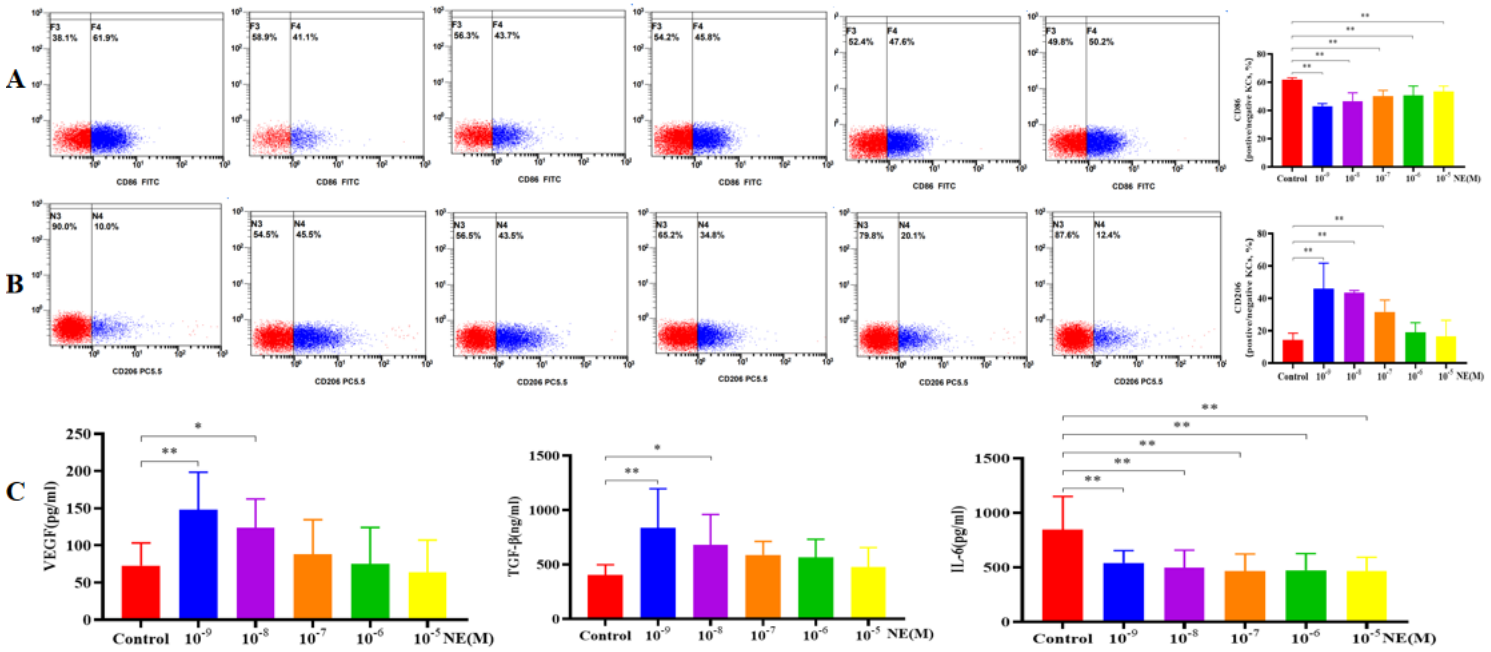

Figure 2

NE induced the M2 polarization of KCs. **A-B**) Effects of NE on KC polarization (CD86 is a marker of M1 KC polarization and CD206 is a marker of M2 KC polarization; n=6); **C**) Effects of NE on KC secretion (IL-6 is a cytokine secreted by M1 KC, while VEGF and TGF-β are cytokines secreted by M2 KC; n=8).

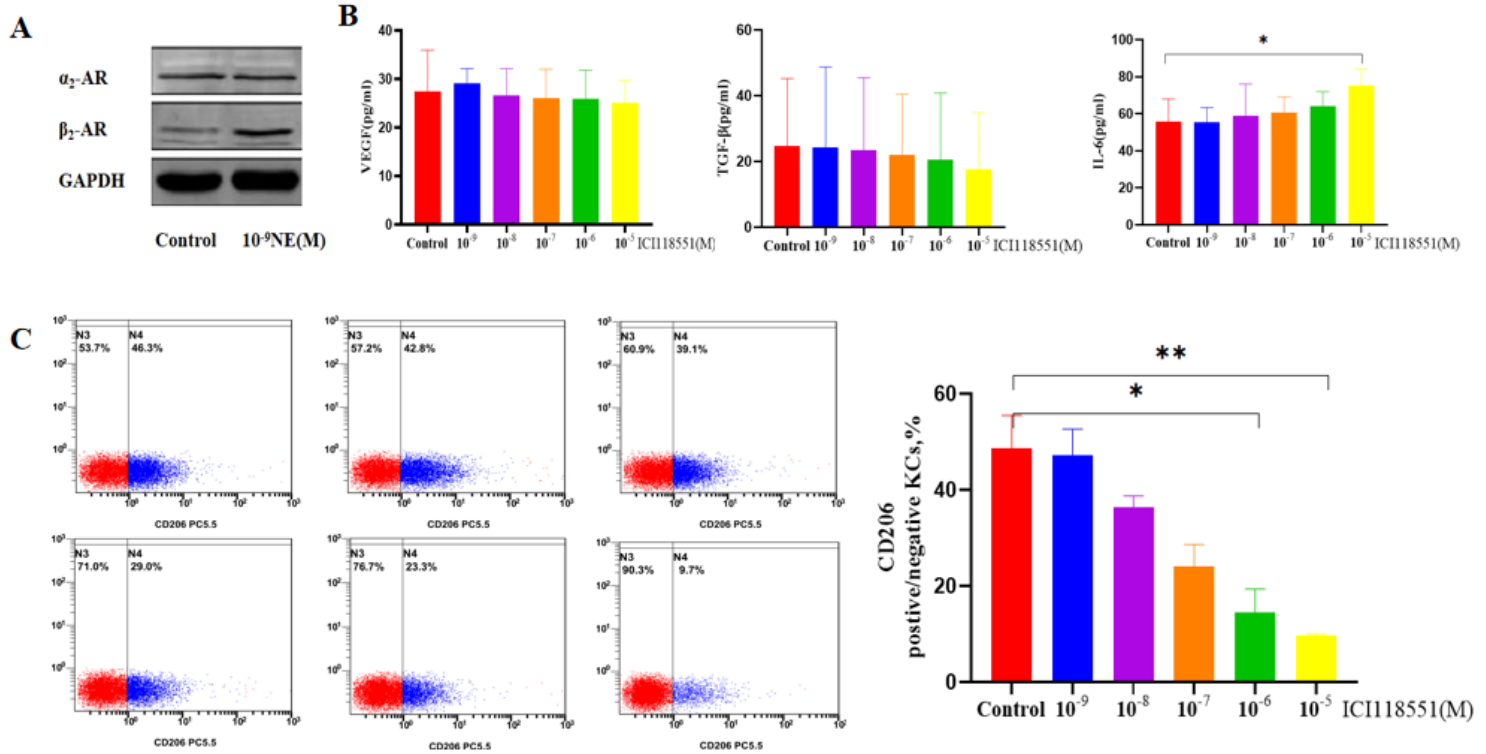

Figure 3

NE affects KC polarization via β_2-AR on the surface of KCs. **A**) Expression of receptors on the surface of NE-treated KCs; **B**) Effects of NE on KC polarization after addition of a β_2-AR blocker (CD206 is a marker of KC M2 polarization; n=6); **C**) Effects of NE on KC secretion after addition of a β_2-AR blocker (IL-6 is a cytokine secreted by M1 KC, whereas VEGF and TGF-β are cytokines secreted by M2 KC; n=8).

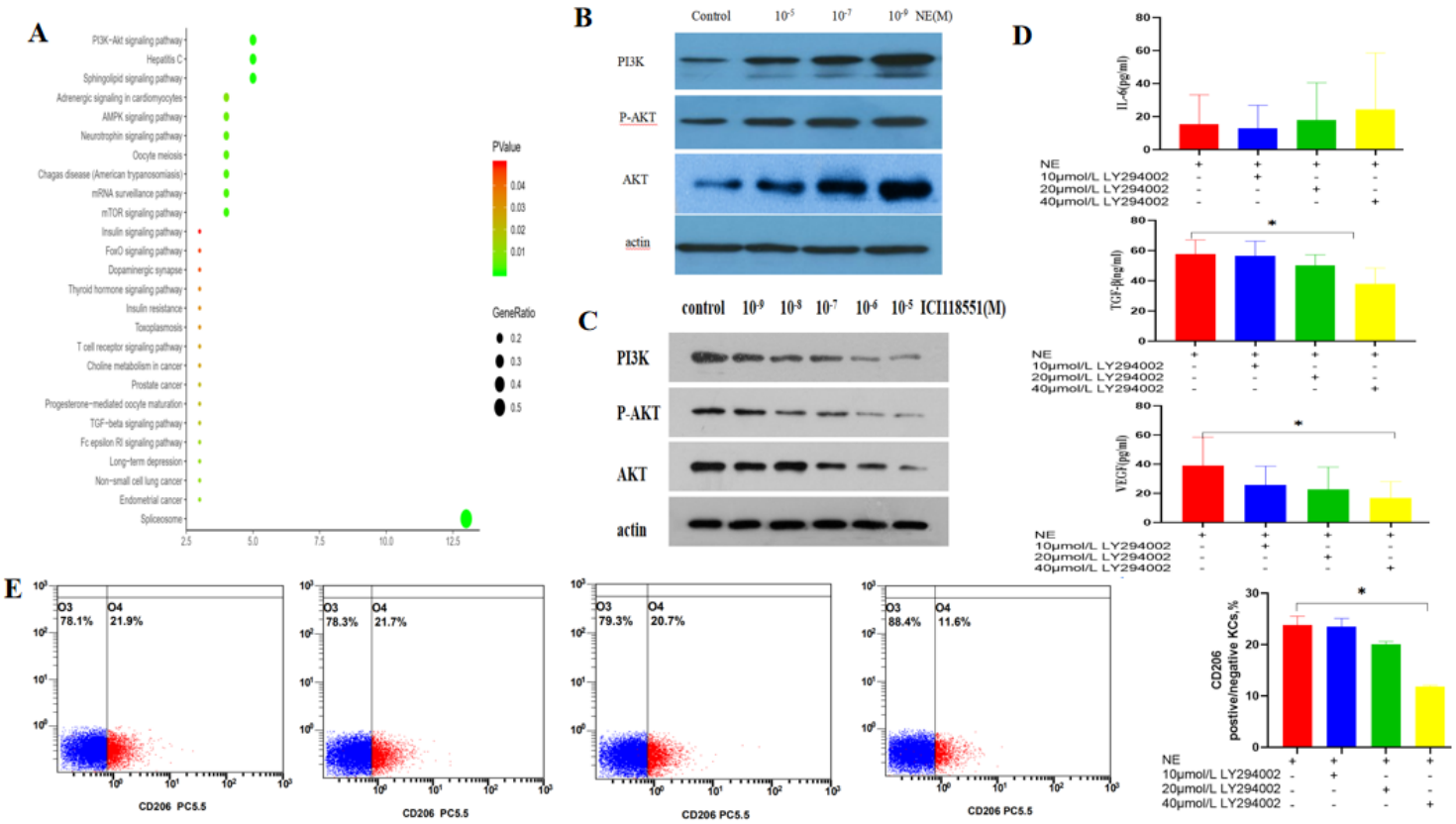

Figure 4

NE affected KC polarization and function by activating PI3K/Akt pathway. **A**) GO and KEGG pathway enrichment analysis of differential genes in CRC non-liver metastasis samples and liver metastasis samples; **B**) Effect of NE on the expressions of PI3K, PAN-Akt, and p-Akt proteins; **C**) Effect of NE on PI3K, PAN-Akt, and p-Akt protein expressions in KCs after addition of a β2-AR blocker; **D**) Effect of NE on KC secretion after blocking the PI3K/Akt pathway (IL-6 is a cytokine secreted by M1 KC, while VEGF and TGF-β are cytokines secreted by M2 KC; n=8); **E**) Effect of NE on KC polarization after blocking the PI3K/Akt pathway (CD206 is a marker of KC M2 polarization; n=6).

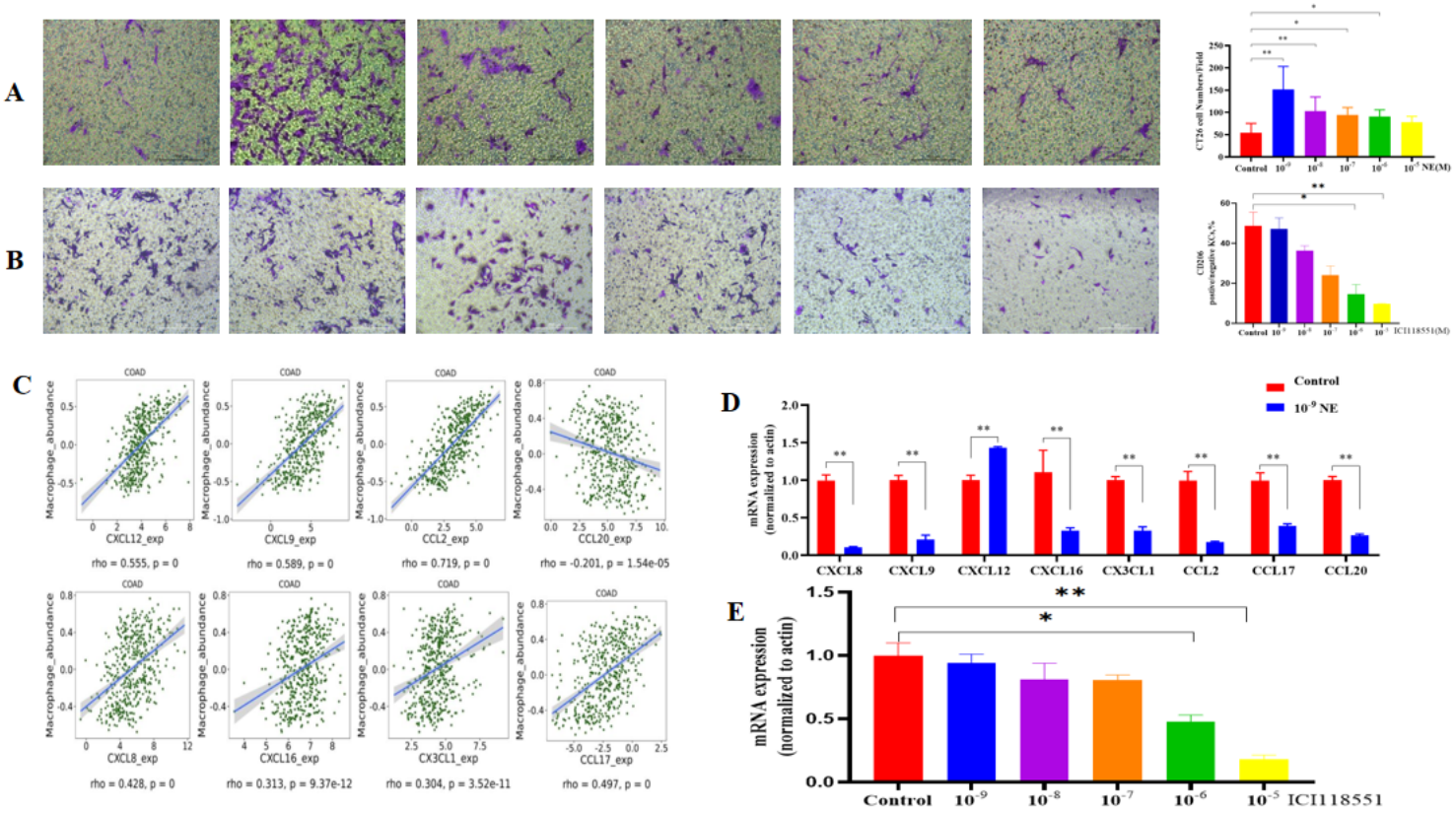

Figure 5

M2 KC promoted the directional migration of CT26 cells via CXCL12. **A**) Effect of M2 KC on the migration of colon cancer CT26 cells; **B**) Effects of KC on the migration of colon cancer CT26 cells after adding a β2-AR blocker; **C**) Eight macrophage-associated chemokines screened from the TISIDB website; **D**) Effects of low concentration (10^{-9} M) of NE on the expressions of CXCL12, CXCL9, CCL2, CCL20, CXCL8, CXCL16, CX3CL1, and CCL17 in KCs; and **E**) Effects of low concentration (10^{-9} M) of NE on CXCL12 expression in KCs after adding a β2-AR blocker.

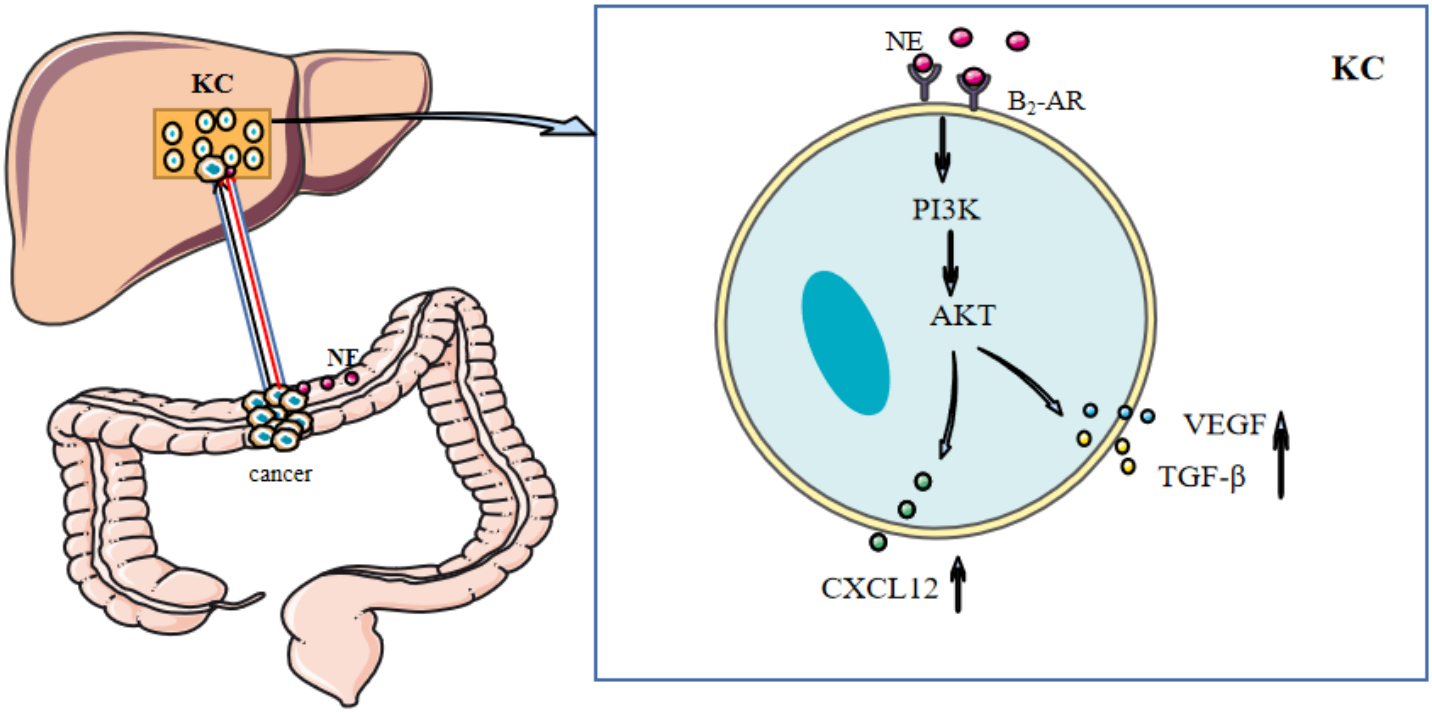

Figure 6

NE/β_2-AR may induce intrahepatic KC M2 polarization through the PI3K/Akt pathway and promote its secretion of CXCL12 to induce the directional migration of CRC to the liver.